Appendix-C1

Severe Accident Analysis Report for DCH

TABLE OF CONTENTS

LIST OF TABLES

LIST OF FIGURES

1.0 INTRODUCTION

The phenomena of HPME and DCH were first considered in the Zion Probabilistic Safety Study (ZPSS) (Reference 1). Until this time, analyses, such as those in the Reactor Safety Study (Reference 2), considered that if the reactor vessel should fail as a result of a severe core damage event, the molten core debris would reside in the reactor cavity. In the ZPSS, it was considered that the spectrum of accident sequences could potentially result in a situation wherein the RPV would fail due to high temperature core debris in the lower plenum and with the RCS at a significant pressure. As a result, the core debris would be initially released to the reactor cavity, but the subsequent blowdown of saturated water, steam and hydrogen from the RCS could displace, push, and entrain the core debris out of the reactor cavity to other regions of the containment. In the ZPSS it was also considered that this high temperature core debris could potentially heat the containment atmosphere.

Subsequent to this study, numerous experiments were performed to determine if dynamic removal of core debris from the reactor cavity would occur should the RPV fail under significant pressure. These experiments, summarized in this report, demonstrate that high density, high temperature melt could indeed be dynamically removed from various types of reactor cavities for situations in which the RCS pressure was greater than approximately 2 MPa at the time of RPV failure. Since this covers a spectrum of accident conditions, dynamic removal was considered in more depth with respect to its potential for directly heating the atmosphere. Hence, the issue of DCH was identified and was the central focus of numerous studies, both analytical and experimental. In the next section, the key experiments that have added to the knowledge base and led towards resolution of this issue for USA cavity designs with large instrument tunnels are described. The section ends with a review of the DCH experiments directed at providing data for European-type reactor designs. Most of these experiments relate to dispersal of molten debris from the reactor cavity and the potential for heating of the containment atmosphere.

The successful DCH modeling tools are reviewed in section 3. The first successful modeling tool for DCH model is CLCH (Convection Limited Containment Heating) model (Reference 35) which is described in section 3.1. The key argument of CLCH model is that the heat transfer between the melt and the gas is limited by the amount of blow-down gases that have intimate (coherent) contact with the melt. Once the melt particles are trapped and deposited in the subcompartment, the heat transfer between the melt and the containment atmosphere becomes negligible, and the major energy addition into the atmosphere is through the combustion of the so-called pre-existing hydrogen. The other modeling tool for DCH is TCE (Two-Cell Equilibrium) model (Reference 36) which is described in section 3.2. The TCE model is another model used to assess the DCH risk, which is an extension of the SCE (Single-Cell Equilibrium) model to account for the effect of containment compartmentalization. The detailed information for TCE model is provided in section 3.2. Section 3.3 is described the accident scenarios used for DCH analysis. These scenarios are selected based on the NUREG/CR-6075, Supplement 1 (Reference 35).

The application of DCH analysis to APR1400 is described in section 4. Section 4.1 is described the assessment of melt transport toward upper compartment. This section is included the interpretation on the behavior of the corium in the reactor cavity applying APR1400 design. Section 4.2 is described the actual methodology used in DCH analysis for APR1400.

An assessment result on the APR1400 containment to DCH effects is described in section 5. The assessment was performed using TCE model with selected accident scenarios in section 3.3. According to the assessment result, APR1400 meets the success criterion established in NUREG/CR-6338 (Reference 46), where DCH problem is considered resolved if Conditional Containment Failure Probability (CCFP) is less than 1% (0.01).

2.0 REVIEW ON THE EXISTING EXPERIMENTS

2.1 Sandia High Pressure Melt Streaming (HIPS) Experiments

The Sandia HIPS experiments (Reference 3) were conducted to confirm the dispersal of debris from a simulated cavity geometry and to assess the phenomena of jet geometry, gas solubility, and aerosol generation (Reference 4). In the tests reported (Reference 5 and 6), a 1:10 linearly scaled model of the Zion cavity was used. This cavity was either open to the atmosphere or placed within an expansion chamber with one end open to the atmosphere. No attempts were made to maintain the geometric similarity of containment internal structures of Zion for these experiments. Iron-alumina thermite charges with masses of about 80 kg were used. A table of reported tests presented in Pilch and Tarbell is reproduced here in Table 2-1.

Table 2-1 Selected HIPS Experiments

Test Name	Scale	Thermite Mass		Initial Vessel Pressure		Extent Dispersal (%)	Water In Cavity
		(kg)	(lbm)	(MPa)	(psia)		
SPIT-19	1:20	10.3	22.7	12.6	1827	95	No
HIPS-2C	1:20	80.0	176	11.7	1697	99	No
HIPS-4W	1:10	80.0	176	11.7	1697	~95*	Yes
HIPS-5C	1:10	80.0	176	6.7	972	99	No
HIPS-6W	1:10	80.0	176	3.8	551	~95*	Yes
HIPS-7C	1:10	81.5	179	5.5	798	98	No
HIPS-8C	1:10	80.0	176	3.7	537	98	No
* Cavity destroyed during test.							

In experiments HIPS-7C and -8C carbon dioxide was used as a cover gas, at pressures between about 3 MPa and 5.6 MPa. Pressures as high as 11.7 MPa were used in two other tests (HIPS-2C and -4W). In two reported experiments (HIPS-4W and -6W), a water-filled cavity was used and destroyed by overpressure during the blowdown due to the small amount of space available for gas expansion. One experiment (HIPS-8C) featured an annular gap around the thermite generator, simulating the gap around the RPV if the insulation were assumed to be removed. During all the HIPS tests, dense aerosol clouds surrounded the debris jet, and sweepout from the cavities was nearly complete in all cases, above 95%. After tests in which the cavity was placed inside the confinement room, this debris was found either within the room or on the concrete pad just outside its open end. This test series demonstrated the substantial influence of structures to capture the debris outside of the reactor cavity/instrument tunnel.

In the HIPS-7C tests, over 30% of the debris was found in the rear of the confinement chamber, much of it against the rear wall. Observations with high speed films show debris exiting the cavity splashing off the ceiling and raining down in that location. Over 97% of the original melt mass was recovered from the chamber and concrete pad, and the rest either landed on the ground beyond the

pad or was in the aerosol cloud which billowed out. Thus, the confinement chamber does not model the containment lower compartment structures. On the other hand, it does illustrate that a minimal representation of the structure results in substantial removal of the debris from the gas stream.

In the HIPS-8C tests, aluminum collection pans were placed on the chamber floor to determine the spatial distribution of debris exiting the cavity, and deduce which fraction exited through the keyway outlet, and which fraction exited through the angular gap around the melt generator. About 25% of the debris was concluded to have been released through this gap, deflected off the ceiling, and fallen into pans around the melt generator. This corresponds to the area fraction taken up by the annular opening.

2.2 Argonne Wood's Metal Tests

The influence of the containment configuration outside the reactor cavity and instrument tunnel was demonstrated by the isothermal Wood's metal experiments (Reference 7). In these tests, the Zion reactor cavity-instrument tunnel configuration was mocked-up along with the seal table and biological shield inside the crane wall (missile barrier). Wood's metal, which has a melting temperature of 73°C and a density of about 9500 kg/m^3, was used to simulate the debris. The experimental configuration is illustrated in Figure 2-1, and the experimental conditions are summarized in Table 2-2. As shown in the table the parameters investigated included various masses of water initially accumulated within the reactor cavity as well as different gas velocities through the cavity following molten metal discharge from the simulated reactor vessel.

The final debris configuration was reported in terms of (1) the material left within the reactor cavity, (2) that which was dispersed within one equivalent diameter of the instrument tunnel exit, and (3) that fraction of debris dispersed beyond one equivalent diameter of the instrument tunnel. High speed movies showed a large fraction of the debris is initially transported as a large wave moving along the outer sloping surface of the instrument tunnel, impacting upon the bottom surface of the seal table. The results demonstrate the structure in the lower compartment is very effective in separating the debris from the high velocity gas stream and depositing the debris on the containment floor in close proximity to the instrument tunnel. More specifically, the structure has a first order effect on the debris distribution in the simulated containment.

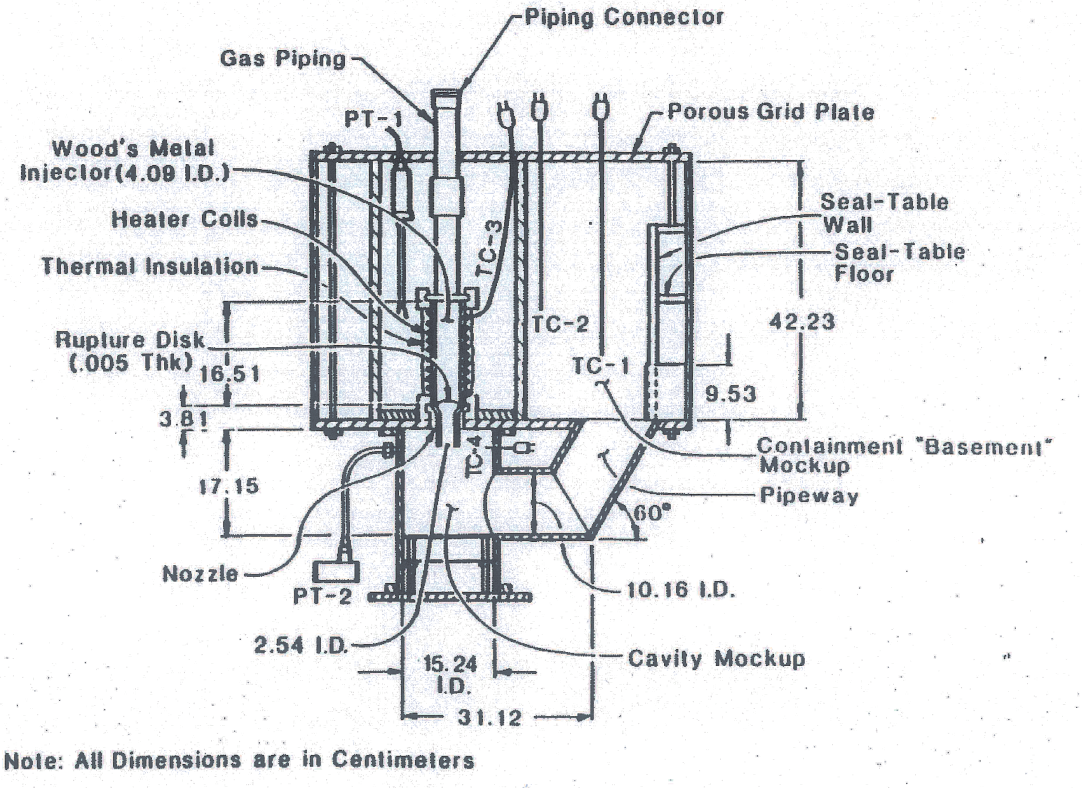

Figure 2-1 Sectional view of the experimental apparatus for the ANL Wood's metal tests

Table 2-2 Summary of Wood's Metal Injection/Dispersal Tests

Test Number (Old Ref.)	**1 (17)**	**2 (18)**	**3 (19)**	**4 (20)**	**5 (21)**	**6 (22)**	**7 (24)**	**8 (25)**	**9 (26)**	**10 (27)**	**11 (28)**
Injected Material (1)	Gas Only	WM	WM	WM	WM	WM	WM	WM	WM	WM	WM
Cavity Water Level, h/D_t (2)	0.5	Dry	0.1	0.1	0.5	1.0	0.1	0.1	0.5	1.0	Dry
Injector Temperature, °C/°F	--	89/192.2	91/195.8	75/192.2	89/192.2	90/194	89/192.2	88/190.4	87/188.6	88/190.4	89/192.2
Injection Pressure, MPa/psia	0.65/94.25	0.70/101.5	0.68/98.6	(3)	0.55/79.75	0.68/98.6	0.68/98.6	0.30/43.5	0.25/36.25	0.25/36.25	1.40/203
WM Injection Velocity, m/s/ft/s	7.8/25.57	7.8/25.57	7.8/25.57	7.8/25.57	7.8/75.57	7.8/25.57	7.8/25.57	5.4/17.70	5.4/17.70	5.4/17.70	11.7/17.70
Gas Velocity (4″ pipe), m/s/ft/s	28/91.80	29/95.08	27/88.52	28/91.80	27/88.52	29/95.08	9.7/31.80	9.3/30.49	9.3/30.49	9.4/30.82	35/114.75
Maximum Cavity Pressurization, kPa	--	10	35	20	80	190	33 (4)	10	60	120	50

NOTES: (1) WM = Woods Metal (T_{mp} = 73°C).
(2) D_t = pipeway diameter, 10.2 cm.
(3) WM frozen in PT standoff line.
(4) High pressure caused cavity apparatus to rupture at 60° pipe elbow.

2.3 Argonne Corium/Water Thermal Interaction (CWTI) Tests

The CWTI series of reactor material DCH experiments were performed by Spencer et al., Spencer et al. and Spencer, et al. (Reference 8, 9, and 10). The experimental configuration represented some major features of the Zion reactor lower containment compartment cavity, and the upper compartment at a 1:30 linear scale. Reactor materials (principally UO_2 and stainless steel) were used and created by an exothermic thermite reaction. Molten debris was injected downward into a simulated cavity and keyway (see Figure 2-2), connected to an expansion volume partitioned like the lower and upper compartments of a containment. In some tests, water was present either in the cavity or the expansion volume or both. The objectives of these tests were to examine heat transfer between core debris and water, sweepout of water and core debris from the cavity, steam generation, hydrogen generation, and to characterize the spatial distribution of dispersed debris.

The test apparatus included the thermite reaction vessel (the source of the molten core debris), an interaction vessel (representing the reactor cavity), a pipe simulating the instrument tunnel, an expansion vessel representing the containment, a "trap" above the pipe discharge to simulate a seal table and a baffle plate to separate the expansion vessel into upper and lower compartments. It is noted that the geometric similarity of the simulated cavity was somewhat distorted (from the Zion cavity design) because of the use of a 90°-bend circular pipe as a keyway instead of a 64°-bend rectangular duct. The simulated core debris produced by the thermite reaction was composed of 60% UO_2, 16% ZrO_2, 24% stainless steel (67% Fe, 21% Cr, 12% NI) and had a temperature of about 3100 K.

Tests were performed with low (less than 0.5 MPa) and high (~ 5 MPa) pressure blowdowns as well as with inert and oxidizing atmospheres. Several different initial water level conditions were tested in the interaction vessel ranging from completely empty to essentially full of water before the melt was released from the thermite furnace. Initial conditions and results for DCH-related CWTI tests are listed in Table 2-3.

The DCH-related tests were conducted by starting the thermite reaction at nominally atmospheric pressure. The melt was subsequently pressurized (by gas from external high pressure gas cylinders) to burst a bottom diaphragm and initiate melt ejection. The duration of the gas blowdown was sufficiently long to assure sweepout of all available melt. Debris not swept out remained as a 1 ~ 3 mm thick crust uniformly deposited on the wall of the interaction vessel and the entire pipe surface (for CWTI-5 and -6).

Various mass fractions of debris were observed to be dispersed from the reactor cavity into the simulated containment volume. Debris was collected at various locations in the apparatus including (1) the interaction vessel and pipe, (2) the "particle trap reflector" at the top of the pipeway as it exited into the bottom of the expansion vessel, (3) on the floor of the simulated containment, and (4) on the top of the simulated lower compartment representing the operating deck. Characteristic particle sizes for the particles swept out into the air atmosphere ranged from 64 to 700 microns for tests CWTI-11 and -13, which had no water in the cavity. Most particles were in the range 100 ~ 300 microns. The experiments with water in the interaction vessel or expansion volume prior to melt ejection demonstrated the effectiveness of water for removing heat from dispersed debris, including the energy released due to oxidation. These tests exhibited little or no direct containment heating. Results for test CWTI-12 show no significant contribution to DCH with

the co-dispersal of debris and water into the containment atmosphere. Test CWTI-12 was performed without the presence of the impeding structure and clearly demonstrates the influence of co-dispersed water. Modest direct containment heating was observed in tests CWTI-6 and -11 which had water only in the pan of the expansion vessel (containment floor). The largest atmospheric heating occurred in test CWTI-13 where no structures and no water were present in either the interaction vessel (cavity) or expansion vessel (containment). This heatup was caused by a sweepout mass of only 0.2 kg. Hydrogen generation and/or oxygen depletion occurring during these tests were also measured to determine the extent of oxidation and its contribution to the overall energy input to the system.

The most important observation from the ANL experiments concerns the influence of structure on debris dispersal. The "particle reflector" in this experiment was a simulation of the in-core instrument tube seal table configuration in a Zion-like containment. The horizontal baffle plate above the "particle reflector" represented the floor separating the Zion containment into upper and lower compartments. Comparison of results from CWTI Tests 6, 11, and 13 reveals the effect of structure on direct containment heating. All three were performed with a dry interaction vessel (reactor cavity), but Tests 6 and 11 included structure in the expansion vessel (containment) while Test 13 had no structure. The DCH efficiencies whose definition is given in Table 2-3 and calculated in reference 10 for Tests 6 and 11 were 5% and 1%, respectively, while the DCH efficiency for Test 13 was reported at 62%. Thus, the substantial effect of the seal table structure was to prevent a significant fraction of the debris from entering the containment atmosphere directly. Because of the structure, a major fraction of the entrained debris was deposited on the lower containment floor.

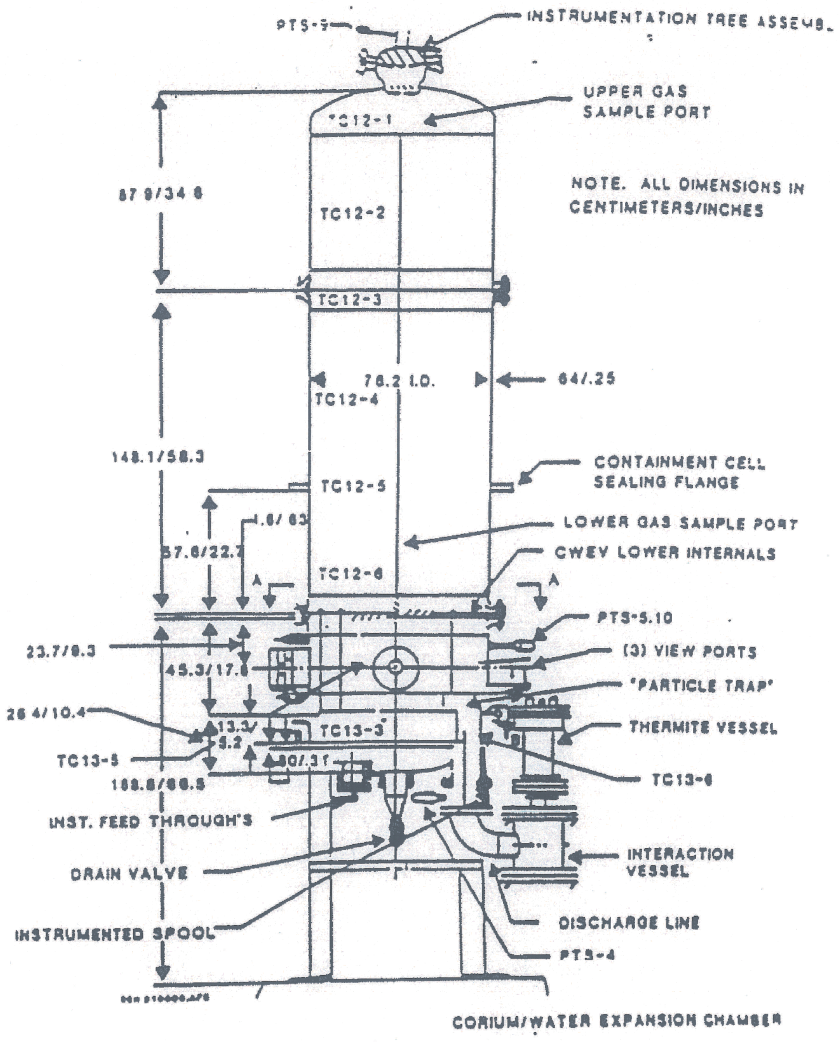

Figure 2-2 ANL thermite apparatus for the CWTI tests

Table 2-3 ANL CWTI DCH-Related Experiments[1]

Test No.	5	6	11	12	13
Driving Pressure, MPa/psia	5.0/725	4.7/681.5	5.1/739.5	2.8/406	4.0/580
Atmosphere	AR	AR	air	air	air
Corium Mass Injected, kg/lbm Corium Mass Swept Out, kg/lbm	3.94/8.67 2.44/5.37	3.75/8.25 1.21/2.66	2.93/6.45 0.88/1.94	2.69/5.92 1.31/2.77	2.27/4.99 0.20/.44
Corium Mass Remained, kg/lbm	1.5/3.3	2.54/5.59	2.05/4.51	2.38/3.04	2.07/4.55
Water in Cavity, kg/lbm	5.6/12.32	dry	dry	4.6/10.12	dry
Dispersal Impediments	s/b[2]	s/b	s/b	none	none
Atmosphere Initial Temp, K/°F	419/294.2	408/274.4	411/279.8	422/299.6	298/76.4
Atmosphere Peak Temp, K/°F	417/290.6	461/369.8	435/523	407/272.6	621/657.8
Atmosphere Initial Pressure, MPa/psia	0.52/75.4	0.22/31.9	0.22/31.9	0.37/53.65	0.32/46.4
DCH Efficiency, %	0	5	1	0	62

[1] 3.33 % linear scale model of Zion.

[2] s/b - shroud/baffle.

[3] DCH efficiency = $\frac{\text{Measured Atm. Heatup}}{\text{Max. Equilibrium Atm. Heatup}}$ x 100.

2.4 Sandia Surtsey Experiments (Initial)

A series of experiments designated as Surtsey was conducted at Sandia (Reference 11, 12, 13, 14, and 15). Experiments DCH-1, 2, 3 and 4 used cavity configurations similar to those of the HIPS 1:10 linear-scale Zion mockups. These cavities were completely enclosed in a large expansion vessel (called SURTSEY) of 103 m^3 capacity and a 1.0 MPa design pressure. No attempts were made to represent the geometry of the Zion containment internal structures such as the seal table, the lower compartment, the operating deck, etc. Four tests were performed, and results were presented in the detailed reports referenced above.

DCH-1 involved 20 kg of molten iron-alumina thermite injected into a 1:10 linear scale model of the Zion cavity only, with a nonprototypic exit guide box added to the instrument tunnel exit to direct debris upward along the centerline of the vessel. Figure 2-3 illustrates the Surtsey facility (Reference 16). The thermite was propelled with nitrogen gas initially at 2.55 MPa. Peak pressures ranged from 0.09 MPa to 0.13 MPa and were achieved less than one second after debris dispersal. High speed film shows debris shooting upward at 40 m/s, expanding laterally and filling the entire chamber cross-section within a few meters of the cavity exit. About 11.6 kg were dispersed from the cavity, including the correction for estimated oxidation. Melt retained within the cavity and chute was in the form of a thin crust, and a 1.2 kg mass was found at the base of the keyway inclination. Aerosol measurements indicated that much material was fragmented to a size under 10 microns, but the measurements may be inaccurate and a large uncertainty is present in the actual amount of such material. The calculated range of aerosolized debris was 5 to 25% of the dispersed mass. Mechanical sieving of debris collected in the chamber showed a log-normal size distribution with a mass mean size of 0.55 mm. Thus the bulk of the debris ejected from the

cavity was of millimeter size. This test was analyzed using the methodology described in Henry (Reference 17) and good agreement was obtained when the specific configuration without structure was considered.

DCH-2 involved 80 kg of molten iron-alumina thermite injected into a 1:10 linear scale model of the Zion cavity and instrument tunnel only, with a nonprototypic exit guide box added to the exit to direct debris upward along the centerline of the vessel. The thermite was propelled with nitrogen gas initially at 6.77 MPa and peak pressures ranged from 0.22 MPa to 0.31 MPa and were achieved less than one second after debris dispersal. High speed film showed that debris leaving the guide box expanded laterally and filled the entire chamber cross-section within a fraction of a second, likely indicating the debris-gas two-phase mixture was "choked" at the exit of the guide box. The total mass recovered from the test chamber, cavity, and melt generator was about 99.5 kg, representing an increase in mass above that injected of 24%. This was attributed to several potential sources related to the construction of the apparatus and test conduit as well as oxygen uptake by oxidation of the iron in the thermite. The latter source was considered to be the most dominant mechanism. About 91.3 kg were dispersed from the cavity. Five types of debris were identified, with each type being generally associated with a particular area of the apparatus. On the upper third of the vessel in line with the cavity exit, 1-2 mm thick sheets of brittle debris were tightly bonded to the wall. Debris stuck to lower portions of the vessel wall was loosely bonded and formed sheets of 2-4 mm thickness. On horizontal surfaces, debris was found to be approximately 1-mm diameter spheres, and agglomerations of such spheres with irregularly-shaped masses of previously molten debris. Melt retained within the cavity and chute was in the form of a thin crust, and a 2 kg mass was found directly underneath the melt generator. This test was also analyzed using the methodology proposed by Henry and found to be consistent with the methodology considering the simplified geometry used in the experiment.

DCH-3 and DCH-4 have been fully reported. The overall results of Tests DCH-1 to DCH-4 are summarized in Table 2-4. Test DCH-1 had the largest efficiency of energy transfer from the debris to the atmosphere (> 90%), while the DCH-4 test was lowest with nominally 35%. The latter was affected strongly by the absence of chemical energy release because of the lack of oxygen in the chamber atmosphere. For consumption of oxygen in the chamber, the degree of oxidation in the DCH-1 test was the greatest, while the DCH-3 debris was the least oxidized.

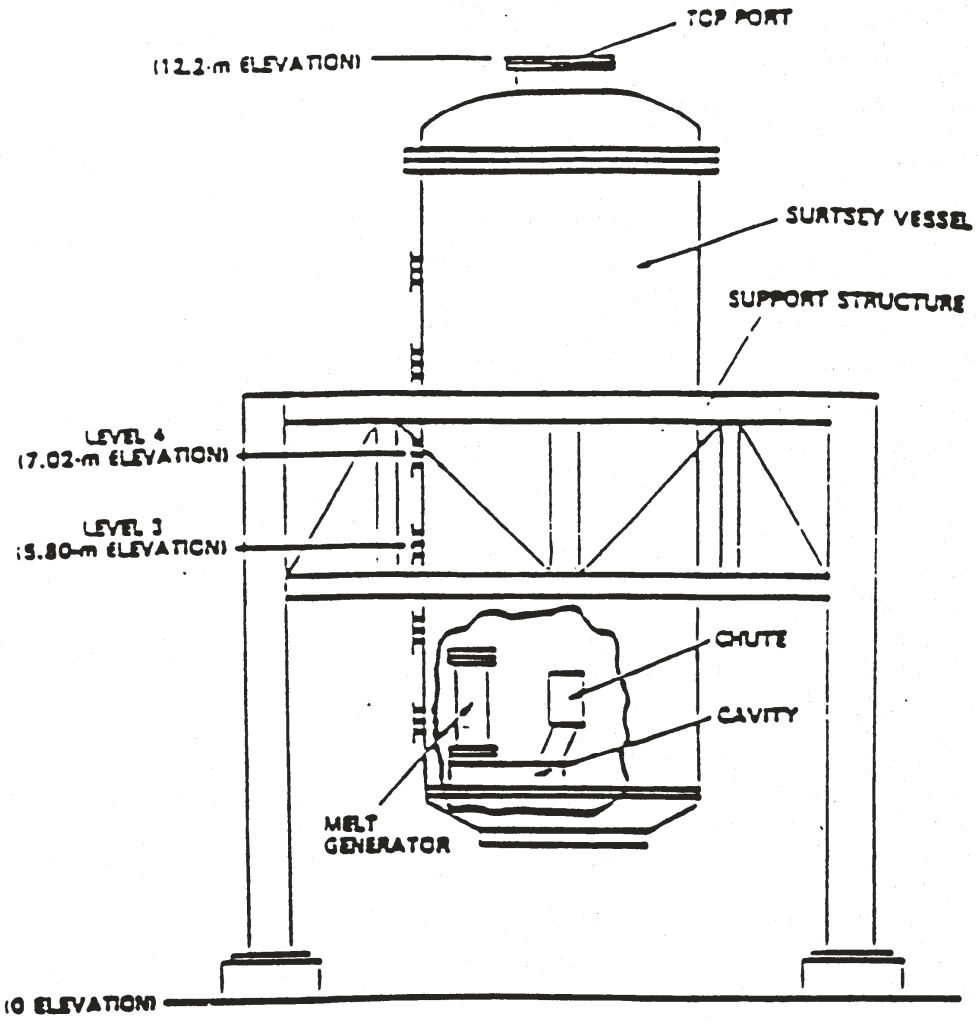

Figure 2-3 Schematic of the Surtsey Direct Heating Test Facility

Table 2-4 SNL-DCH Experiments[1,2]

Test	Driving Pressure MPa/psia	Driving Gas	Thermite Mass (kg/lbm)			Peak Temp °C/°F	Peak Press MPa/psia
			Initial	Swept-Out	Remained		
DCH-1	2.4/348	N_2	20/44	~10/22	~10/22	260/500	0.18/26.1
DCH-2	6.8/986	N_2	80/176	~76/167.2	~4/8.8	880/1616	0.33/47.9
DCH-3	6.0/870	N_2	80/176	~75/165	~5/11.0	860/1580	0.28/40.6
DCH-4[3]	6.9/1000.5	N_2	80/176	~74/162.8	~6/13.2	860/1580	0.27/39.2

[1] 10% linear scale model of Zion cavity only, no representation of the containment structures outside of the reactor cavity/instrument tunnel.
[2] Dry cavity and containment.
[3] Inert atmosphere.

2.5 Fauske & Associates, Inc. DCH Experiments

The Fauske & Associates, Inc. program addressed the issue of direct containment heating in support of the Zion IPE (Reference 18). In keeping with lessons learned from smaller scaled tests, these experiments were conceived and designed to have a 5% linear scale simulation of the reactor cavity, instrument tunnel, lower compartment (including two steam generators, two reactor coolant pumps and the refueling canal wall) and upper compartment of the Zion containment building. Figure 2-4 and Figure 2-5 show the experimental apparatus and Figure 2-6 describes how the experiment represents the reactor containment. Iron-aluminum thermite was used to simulate the molten core material, with the 20 kg thermite mass representing about twice the scaled debris mass and energy content of the Zion reactor. This was done to compensate for the greater propensity of freezing on the reactor cavity walls in small scale experiments. The experiments can also be viewed as a study of the effect of lower containment structures on the dispersal of iron-aluminum debris when compared with the Sandia DCH tests, which also used iron-aluminum as a core material simulant, but had no containment internal structures. This work represents the most complete geometric similarity of the Zion cavity and containment internal structures for the scaled DCH experiments performed to date.

The experimental matrix included four tests, all with 20 kg of thermite, three driven by nitrogen and one by steam. Water was available on the containment floor in all tests and was also available, to different extents, in the various tests; two having about 1 cm of water on the cavity floor, one having 8 cm and the other was performed with a dry reactor cavity. Table 2-5 presents the test conditions for the experimental matrix. Table 2-5 also summarizes the test results and clearly demonstrates that (1) the tests were very similar in their response and (2) very little pressurization occurred in the upper containment compartment. Measurements of the containment pressurization showed very little, if any, contribution to direct heating even though 90% of the material was dispersed. Pressurization in the reactor cavity and instrument tunnel, as well as the lower compartment, was essentially due to debris-water thermal interactions in the reactor cavity, the blowdown of the melt generator, and steam generated in the debris quenching process on the lower compartment floor. The measured peak temperatures of the lower compartment atmosphere were mostly the results of rapid steam generation due to quenching, followed by slow heating of the gas due to debris frozen on structures. This latter energy transfer did not contribute to the pressurization because of the

cooling provided by other heat sinks.

Maximum local DCH efficiency of about 2%, based on the peak pressure, was measured in FAI-DCH-1 where only a limited water mass was present in the reactor cavity before the blowdown. This is an upper-bound estimate of DCH efficiency because the steam partial pressure was conservatively estimated (underestimated). The temperature increase in the lower compartment was about five to six times as high as in the upper compartment but was dominated by the rapid steam generation since the measured peak temperature was only slightly superheated. The results for all four tests were very consistent with respect to the extent of debris dispersed, the peak temperature in the lower compartment and the pressurization transient in the containment. The only differences are the response caused by dynamic interactions in the reactor cavity (determined by the water mass in the cavity) and the hydrogen generated which is a function of the water in the cavity and the driving medium. Given the similarity of the global response for all four tests, these differences have a second order influence on the containment response.

The results were consistent with the Argonne CWTI-DCH tests in that significant heatup of the containment atmosphere was not observed in any runs including the important structural barriers of a seal table and the lower containment compartment. In fact, the capacity of structures to mitigate DCH can be seen by comparing these results to the Sandia DCH results which did not represent these structures. It is to be noted that the use of steam to eject the debris simulant yielded a containment temperature and pressure response virtually identical to the nitrogen blowdown tests, even though more hydrogen was generated, i.e., from 7% to 15% of the metal

Table 2-5 CECo/FAI-DCH Experiments

Test	Driving Pressure (MPa/psia)	Driving Gas	Thermite Mass (Kg/lbm)		Measure Peak Containment Pressure		Water (kg/lbm)	
			Initial	Swept-Out	kPa	Psia	Cavity	Compartment Floor
DCH-1	3.3/478	N_2	20/44	~18/~39.6	165	23.9	1.1/2.4	90/198
DCH-2	2.9/420	N_2	20/44	~18/~39.6	170	24.7	5.3/11.7	47/103
DCH-3	3.2/464	N_2	20/44	~18/~39.6	155	22.5	Dry	47/103
DCH-4	2.3/333	Steam	20/44	~18/~39.6	172	25.0	1.1/2.4	47/103

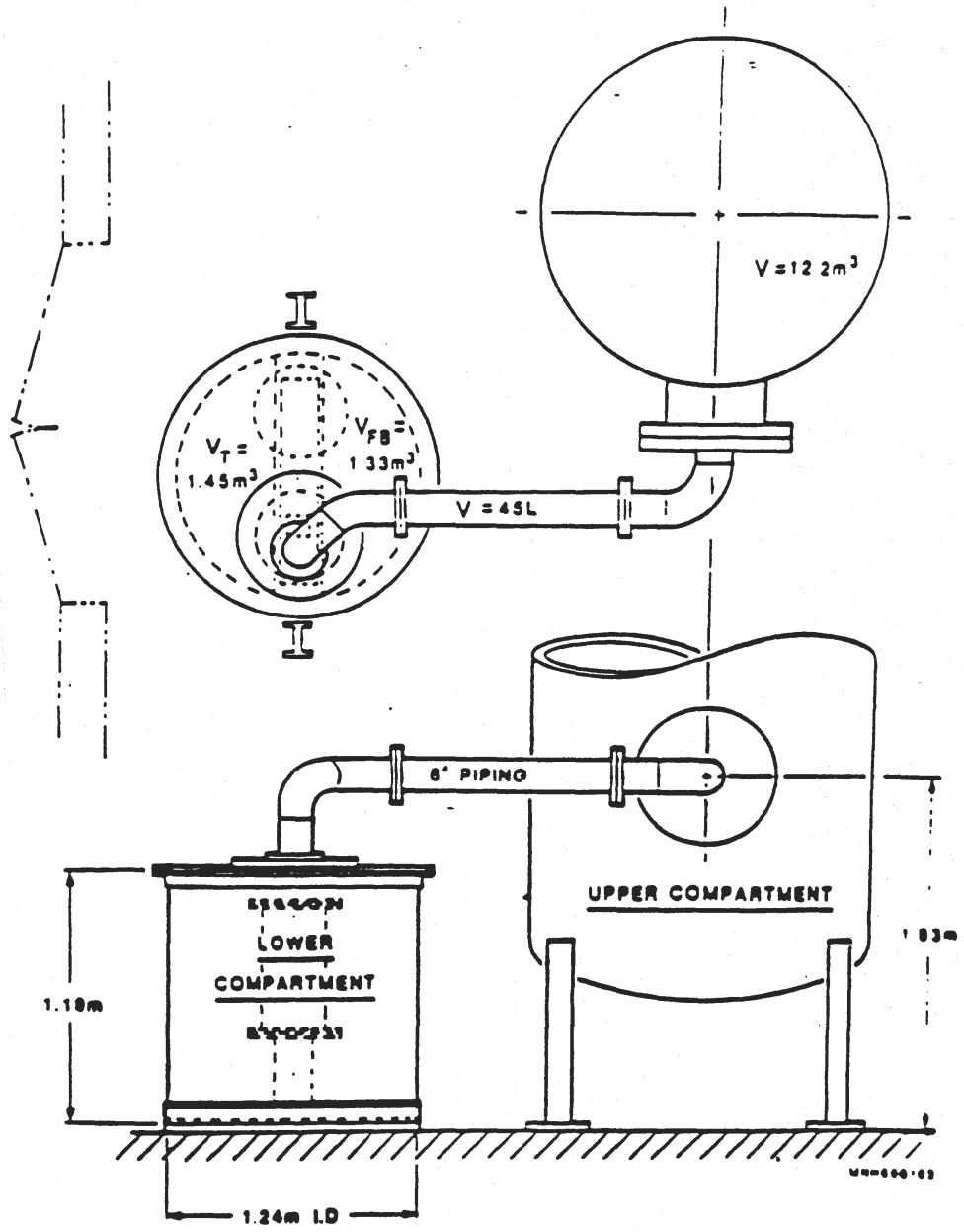

Figure 2-4 Elevation view of the vessel interconnection to simulate the containment configuration

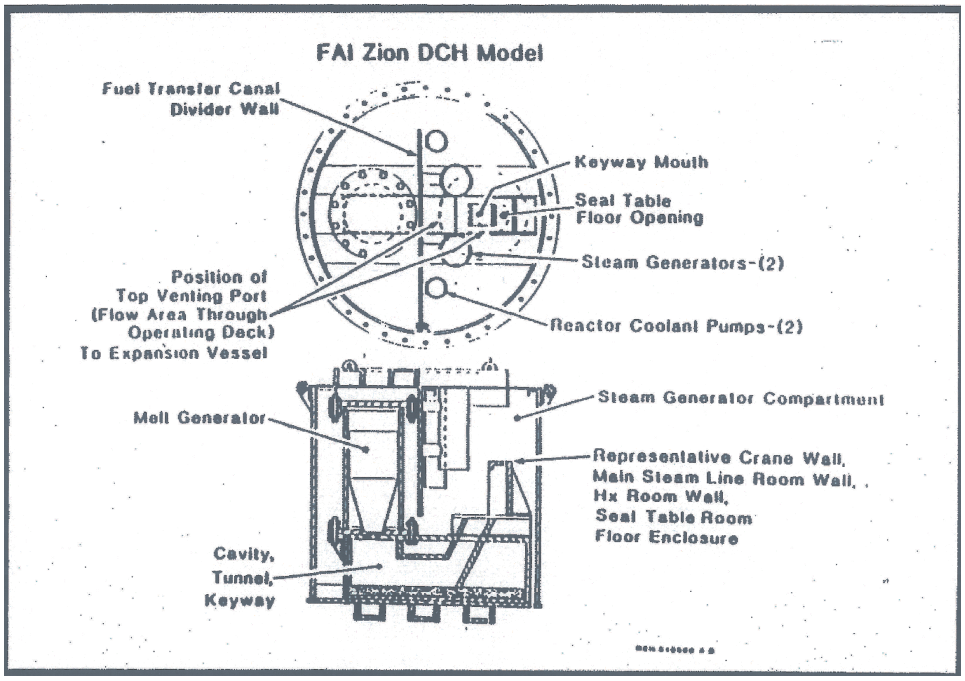

Figure 2-5 **Cross-section of the melt generator, reactor cavity, instrument tunnel and the simulated lower compartment with structures**

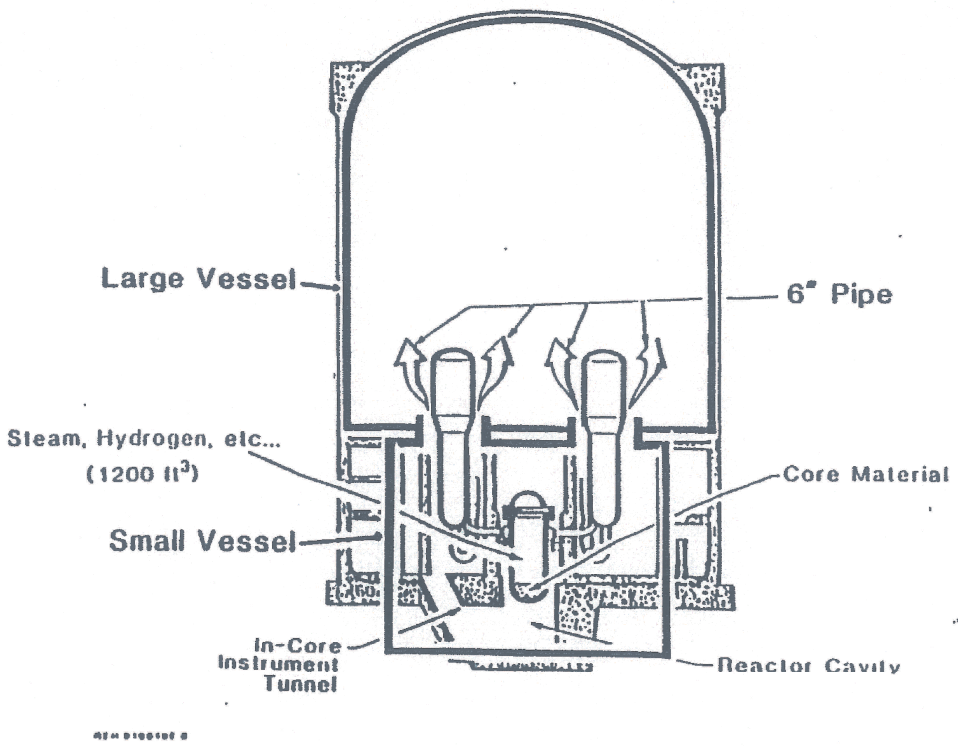

Figure 2-6 Relationship of the test configuration to the Zion containment buildings.